Calculation of Compton Profiles Using a Multipole Expansion of the Momentum Density *

Claudia Blaas and Josef Redinger
Institut für Technische Elektrochemie, Technische Universität Wien

Raimund Podloucky
Institut für Physikalische Chemie, Universität Wien

Peter Jonas and Peter Schattschneider
Institut für Angewandte und Technische Physik, Technische Universität Wien

Z. Naturforsch. **48a**, 198–202 (1993); received December 24, 1991

A practical method for the calculation of Compton profiles for cubic systems with O and O_h symmetry is presented that is based on a multipole expansion of the electron momentum density (EMD) in terms of cubic harmonics. The central quantities, the expansion coefficients, are determined by a Gaussian-type integration (special directions) over the angular coordinates. From these coefficients the coefficients of an analogous expansion of the Compton profile can be directly calculated, establishing a transparent relationship between the electron momentum density and the Compton profile. This direct relationship offers the possibility of tracing back Compton-profile anisotropies to EMD anisotropies more easily, as demonstrated for MgO and FeAl.

Key words: Compton profile; Electron momentum density; Multipole expansion; MgO, FeAl.

1. Introduction

Compton scattering within the impulse approximation [1–4] provides valuable insight into the ground-state electronic structure of solids. The central quantity is the electron momentum density (EMD), which is accessible by summing the squares of the Fourier transforms (FT) of the ground-state one-electron wavefunctions. Unfortunately the Compton profile (CP) contains only the average of the EMD over planes perpendicular to the scattering vector, complicating the interpretation of the CP considerably. It is a very demanding and time consuming task to obtain an experimental EMD, since profiles for many directions of the scattering vector have to be collected. Most of the time one is forced to make a comparison between theory and experiment for CPs or their differences (DCPs) along the main symmetry directions, rather than for the EMD itself. It is therefore highly desirable to gain knowledge of how to relate important features in the CPs (DCPs) to certain features in the EMD. In the present study we try to achieve this goal by noticing that both the EMD and the CPs may be expanded in a series of lattice harmonics, and that the coefficients of both expansions are closely related.

2. Theory

The EMD can be expanded in a series of lattice harmonics (cf. [5] and the references therein), in the present case for the Laue class O_h in a series of cubic (or hexoctahedral) harmonics K_L:

$$n(p,\hat{p}) = \sum_L G_L(p)\, K_L(\hat{p})\,. \tag{1}$$

Unlike in previous work [6, 7] the coefficients G_L (moments of the EMD) are not obtained by least-squares fitting but are computed by integrating over the angular coordinates. We use a Gaussian integration formula (N special directions) introduced by Fehlner and Vosko [8] and also their definition of cubic harmonics:

$$\begin{aligned} G_L(p) &= \int \mathrm{d}\hat{p}\, K_L(\hat{p})\, n(p,\hat{p}) \\ &\simeq 4\pi \sum_{j=1}^{N} A_j\, K_L(\hat{p}_j)\, n(p,\hat{p}_j)\,. \end{aligned} \tag{2}$$

* Presented at the Sagamore X Conference on Charge, Spin, and Momentum Densities, Konstanz, Fed. Rep. of Germany, September 1–7, 1991.

Reprint requests to Dr. Josef Redinger, Institut für Technische Elektrochemie, Technische Universität Wien, Getreidemarkt 9/158, A-1060 Wien, Austria.

0932-0784 / 93 / 0100-0198 $ 01.30/0. – Please order a reprint rather than making your own copy.

Within the impulse approximation [3, 4] the CP is the projection $J_{\hat{a}}(q)$ of the EMD onto the scattering vector $\boldsymbol{a} = |q| \cdot \hat{a}$. Using (1) one gets [9, 10]

$$J_{\hat{a}}(q) = 2\pi \sum_L g_L(q)\, K_L(\hat{a}), \tag{3}$$

$$g_L(q) = \int_{|q|}^{\infty} \mathrm{d}p\; p\; G_L(p)\, P_l\left(\frac{q}{p}\right), \tag{4}$$

where l is the order of the associated Legendre functions P_l^m contained in K_L, and P_l is the Legendre polynomial of the same order.

It is obvious from (4) that the expansion coefficient $g_L(q)$ for a particular cubic harmonic in the CP expansion is based only on the corresponding EMD expansion coefficient $G_L(p)$ (same L-value). This fact is essential to our present work, since it allows us (as we will discuss later on) to trace back anisotropies in the CP (DCPs) to anisotropies in the EMD. Establishing such a link has always been of considerable interest [11–15]. Usually CPs are calculated by a direct numerical integration of the EMD over planes perpendicular to the scattering vector [7, 16, 17]. If the density of sampling points is roughly equivalent, both approaches are of comparable accuracy. However, discussing DCPs in terms of EMD anisotropies is considerably more complicated, if not impossible, in the latter case.

An FT of real-space Bloch wavefunctions and subsequent squaring and summation provides the EMD $n(p, \hat{p}_j)$ along special Gauss-directions $\hat{p}_j$ needed to calculate the expansion coefficients $G_L(p)$. In the present work the wavefunctions have been obtained from a nonrelativistic one-electron Schrödinger equation by means of the Linearized Augmented Plane Wave (LAPW) method [18, 19] within the Local Density Approximation (LDA). The FT of an LAPW wavefunction is similar to the case of an Augmented Plane Wave (APW) wavefunction [7, 16, 20].

Table 1. Parameters for the valence CP calculations.

	MgO	FeAl
Lattice constant [a.u.]	7.96466	5.49619
Number of special directions	15	21
p_{max} [a.u.]	7.33	7.43
Points/direction ($p \le p_{max}$)	651	651
P_{max} [a.u.] – isotropic correction	42.43	41.15
Points/ direction ($p_{max} \le p \le P_{max}$)	90	60
CP-norm in $p \le P_{max}$	7.988	10.998

The procedure outlined above is used to calculate the valence part of a CP. Several additions are necessary to obtain total CPs: (a) isotropic cutoff correction ($p_{max} < \infty$ in (4)), which is essential to achieve the correct normalization, (b) addition of an isotropic atomic-like core-CP, and (c) a Lam-Platzman term [21, 22] to describe electron correlation effects beyond the non-interacting limit, isotropic in the case of the LDA.

3. Computational Details

In order to check the feasibility and accuracy of our approach, we chose two cubic systems as our test cases for which rather accurate theoretical and experimental data exist [16, 17, 23, 24]: Insulating MgO (NaCl structure) and the ordered transition-metal alloy FeAl (CsCl structure). The present LAPW calculation utilizes the same self-consistent LDA muffin-tin potentials [16, 25] as the previous APW calculations and restricts the maximum number of plane waves to 140 for MgO and to 200 for FeAl. The EMD and CPs are computed using the new procedure outlined in Section 2.

The 15- and 21- special-direction Gaussian integration formula [8] was applied to calculate the multipole moments of the valence EMD for MgO and FeAl, respectively. Therefore the first 15 ($L \le 24$) terms for MgO and the first 20 terms ($L \le 28$) for FeAl are described properly both in the EMD and CP expansions. All other parameters are listed in Table 1.

4. Results and Discussion

A) MgO

Figure 1 shows the most important anisotropic contributions to the EMD in the top panel and to the CP in the bottom panel. The $L = 4$ and $L = 6$ contributions ('moments') are of comparable size, whereas the $L = 8$ term (not shown) is already smaller by a factor of 2. For $L \ge 16$ the contributions are practically zero, indicating a rapid convergence of both the EMD and CP expansions. Focussing on the EMD expansion, we find maxima between 1 and 1.5 a.u. It is obvious from Table 2 that the $L = 4$ term transfers momenta from [111] to [100], whereas the $L = 6$ term shuffles momenta from [110] to both [100] and [111]. Hence the net result is a momentum-density transfer

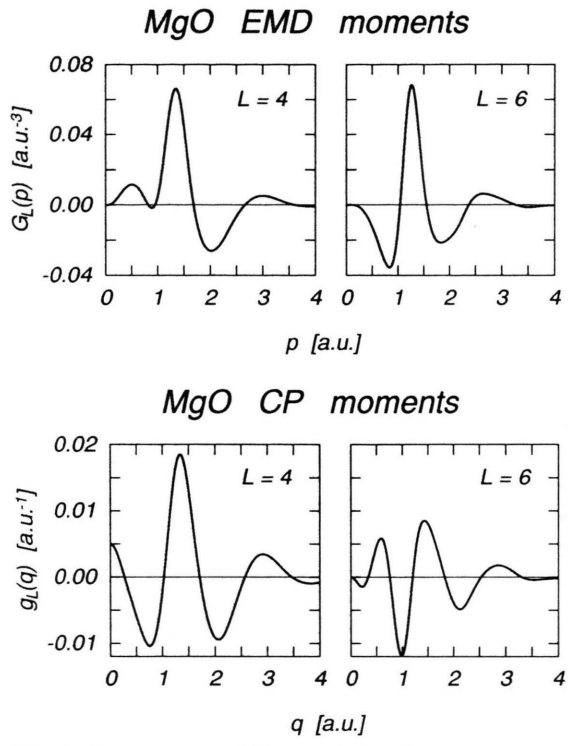

Fig. 1. Expansion coefficients of the electron momentum density (top panel) and of the Compton profile (bottom panel) for MgO.

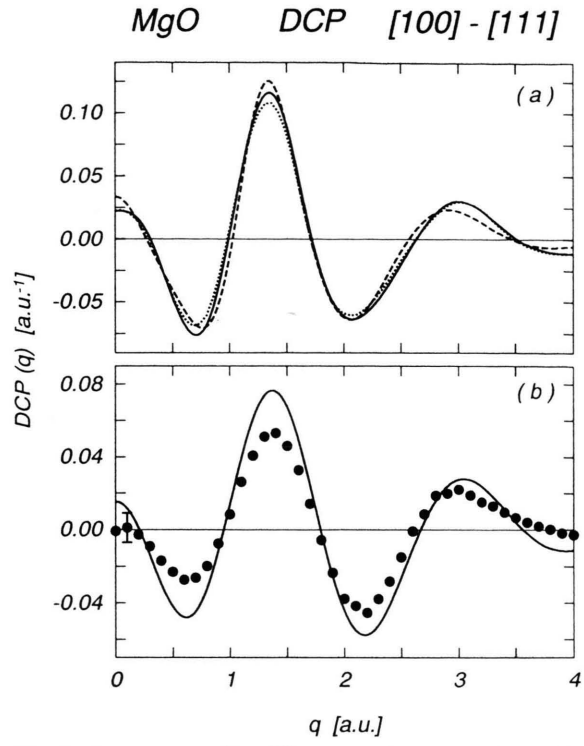

Fig. 2. Compton-profile difference [100]–[111] for MgO: (a) Calculated unconvoluted differences: Total (solid), $L=4$ contribution (dashed), and previous APW results [16] (dotted). (b) Experimental results [23] (bullets) and the present theoretical data convoluted with the experimental residual instrument function (solid).

from [110] (next-nearest neighbours O–O) to [100] (nearest neighbours Mg–O). The redistribution has been attributed to the orthogonality constraints imposed on the ionic O wavefunctions leaking into the Mg-ion core regions [16]. Hence, the $L=4$ and $L=6$ contributions are due to the small components of the wavefunctions around the Mg sites built up by the O wavefunction tails. Considering the CP moments, we see that despite of the integration procedure in (4) the positions of the minima and maxima are similar to the EMD moments.

In Fig. 2a the DCP between [100] and [111] is shown for MgO. Comparing the present results (full line) with those of a previous APW calculation [16] (dotted line), we find a very good agreement. We attribute the small deviations to our denser $\boldsymbol{p}$-mesh and not to the different approaches of computing CPs from the EMD. However, a clear advantage of our present approach is demonstrated by the dashed line in Fig. 2a, indicating that only the $L=4$ contribution matters for this particular DCP (see Table 2). Considering the angular dependence of the cubic harmonics, it is possible to relate the [100]–[111] DCP unambiguously to the different shape of the EMD around the above directions.

Table 2. Values for the cubic harmonics along high-symmetry directions.

L	l	K_L ([100])	K_L ([110])	K_L ([111])
0	0	0.28	0.28	0.28
4	4	0.65	−0.16	−0.43
6	6	0.36	−0.58	0.64

Concerning the agreement with the experimental data [23] shown in Fig. 2b, we refer to the discussion in [16].

B) FeAl

In Fig. 3 we show the EMD coefficients in the top and the CP coefficients in the bottom panel. Although the $L=4$ and $L=6$ terms are the largest, the L-con-

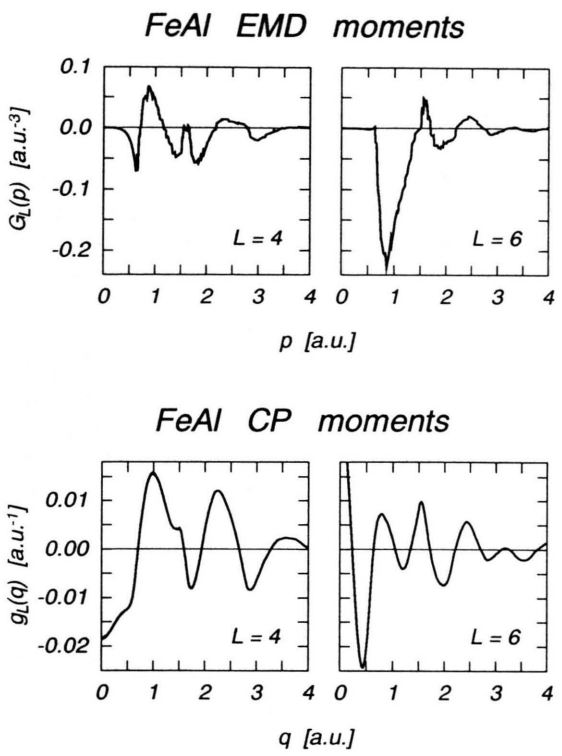

Fig. 3. Expansion coefficients of the electron momentum density (top panel) and of the Compton profile (bottom panel) for FeAl.

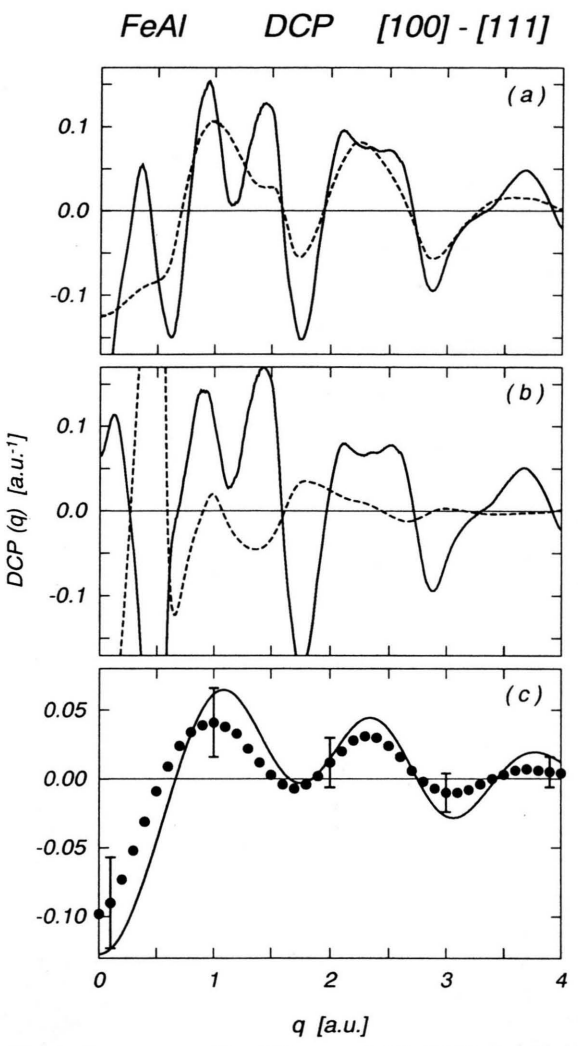

Fig. 4. Compton-profile difference [100]–[111] for FeAl: (a) Calculated unconvoluted differences: Total (solid) and $L=4$ contribution (dashed). (b) Calculated contributions from the lowest Al s-like band (dashed) and from all other, mainly Fe d-like, bands (solid). (c) Experimental results [24] (bullets) and the present theoretical data convoluted with the experimental residual instrument function (solid).

vergence is much slower than for MgO. This is entirely a consequence of the rather complicated Fermi surface, which introduces sharp breaks into the EMD. Yet, we have to disagree with Bross [7], who claimed that a decomposition of the EMD in cubic harmonics is not appropriate, and hence the calculation of CPs will not work properly. Inspecting the EMD moments more closely, we see that the coefficients are smooth only for small p-values (inside the 1st Brillouin zone). The superposed small irregular oscillations are certainly not a consequence of the finite p-mesh along the special directions ($\Delta p \simeq 0.01$ a.u.), but rather of the limited number of special directions, 21 in our case. From the $L=4$ and $L=6$ term we infer a redistribution of the momentum density for $p < 1.5$ a.u. away from the nearest-neighbour direction [111] (see Table 2). The redistribution is mainly caused by orthogonality constraints imposed on the wavefunctions along the Fe–Al bond due to the hybridization of the almost free-electron-like Al states with localized Fe d-states. Looking at the CP moments in Fig. 3 we notice that the small irregular oscillations are smoothed by the integration, leading to a slightly better L-convergence of the CP expansion.

In Fig. 4a we show the [100]–[111] DCP for FeAl, which agrees well with previous APW results [17]. Looking at the contributions from the various terms in the expansion, we find the $L=4$ contribution to be by far the most important one (see Table 2), describing the DCP rather well for $q > 0.75$ a.u. In this region the

DCP is dominated by Fe d-states, which is illustrated in Figure 4b. Anisotropies caused by the localized d-like wavefunctions (e_g vs. t_{2g}) will contribute strongly to the $L=4$ term because the FT step conserves their l-character. At lower momenta we find also a rather large contribution from the lowest almost free-electron-like Al s-band, which is opposite to the Fe d-bands contribution. The opposite sign can be explained by considering orthogonalized plane-wave-like Al states, i.e. states showing a d-like orthogonalization hole around the Fe-sites.

A comparison with most recent experimental results as obtained with a WKα_1-spectrometer [24] is shown in Figure 4c. The agreement is very encouraging, since the remaining discrepancies are contained to a large extent within the present experimental error bars. Nevertheless, the CP anisotropy is overestimated, which seems to be a common feature of all results based on calculations within the framework of the LDA [2].

5. Summary

The present work demonstrates the usefulness of computing CPs via an expansion of the EMD into cubic harmonics. The EMD coefficients are determined accurately by means of a Gaussian-type integration using special directions, which distinguishes our method from the least-squares fitting procedure found in the literature. The CP coefficients are easily obtained from the related EMD coefficients by a one-dimensional integration. This differs from the standard procedure of integrating the EMD over planes perpendicular to the scattering vector and facilitates the understanding of CP anisotropies in terms of EMD anisotropies, as demonstrated for insulating MgO and metallic FeAl. Taking the [100]–[111] DCP as an example, we were able to establish a simple correspondence between CP and EMD anisotropies, even though the origin of the anisotropies is quite different for MgO and FeAl. For MgO, orthogonality constraints are dominating, whereas for FeAl on-site Fe d-like states are identified as a dominant source.

Acknowledgements

We wish to thank Dr. S. Manninen for communicating his experimental data for FeAl prior to publication and Prof. S. G. Steinemann for providing high-quality FeAl single crystals.

The present work was supported by the Austrian Fonds zur Förderung der Wissenschaftlichen Forschung (P7432-PHY) and the Austrian Bundesministerium für Wissenschaft und Forschung (GZ.49.731/2-24/91).

[1] B. Williams (editor), Compton Scattering, McGraw-Hill, New York 1977.
[2] M. J. Cooper, Rep. Prog. Phys. **48,** 415 (1985).
[3] P. M. Platzman and N. Tzoar, Phys. Rev. **A 139,** 410 (1965).
[4] P. Eisenberger and P. M. Platzman, Phys. Rev. **A 2,** 415 (1970).
[5] E. Heuser-Hofmann and W. Weyrich, Z. Naturforsch. **40a,** 99 (1985).
[6] A. Seth and D. E. Ellis, J. Phys. **C 10,** 181 (1977).
[7] H. Bross, J. Phys. **F 12,** 2249 (1982).
[8] W. R. Fehlner and S. H. Vosko, Can. J. Phys. **54,** 2159 (1976).
[9] P. E. Mijnarends, Phys. Rev. **160,** 512 (1967).
[10] P. E. Mijnarends, in [1], p. 323–345.
[11] W. Schülke, phys. stat. sol. (b) **62,** 453 (1974).
[12] F. M. Mueller, Phys. Rev. **B 15,** 3039 (1977).
[13] P. Pattison, N. K. Hansen, and J. R. Schneider, Chem. Phys. **59,** 231 (1981).
[14] N. K. Hansen, HMI-report **B 342** (1980).
[15] N. K. Hansen, P. Pattison, and J. R. Schneider, Z. Phys. **B 66,** 305 (1987).
[16] R. Podloucky and J. Redinger, J. Phys. **C 16,** 6955 (1984).
[17] R. Podloucky and A. Neckel, phys. stat. sol. (b) **95,** 541 (1979).
[18] D. D. Koelling and G. O. Arbman, J. Phys. **F 5,** 2041 (1975).
[19] O. K. Andersen, Phys. Rev. **B 12,** 3060 (1975).
[20] H. Roth-Seefried and H. Bross, Z. Physik **B 26,** 125 (1977).
[21] L. Lam and P. M. Platzman, Phys. Rev. **B 9,** 5122 (1974).
[22] G. E. W. Bauer, Phys. Rev. **B 27,** 5912 (1983).
[23] O. Aikala, T. Paakkari, and S. Manninen, Acta Cryst. **A 38,** 155 (1982).
[24] S. Manninen, private communication (1992).
[25] K. Pechter, P. Rastl, A. Neckel, R. Eibler, and K. Schwarz, Monatsh. Chem. **112,** 317 (1981).